Supplementary Figures

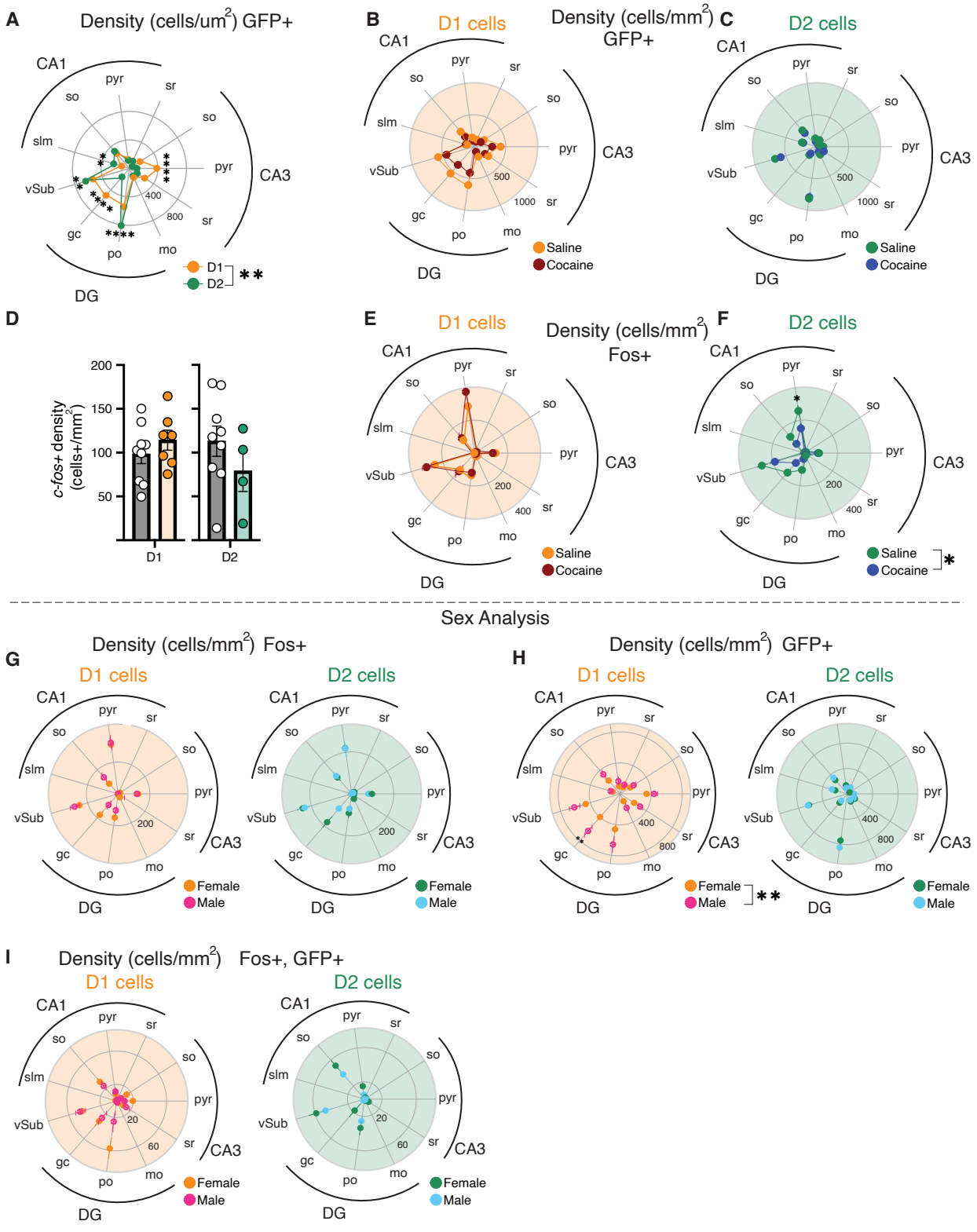

Fig. S1. Sex-specific analysis of FOS+ induction in vHPC D1 and D2 cells following acute cocaine injection.

A) Density of D1 vs. D2-expressing cells (GFP+) across vHPC layers.
B) Proportion of D1 (GFP+) cells following cocaine treatment.
C) Proportion of D2 (GFP+) cells after cocaine.
D) Average FOS+ expression in vHPC after cocaine injection.
E) FOS expression across vHPC layers in D1 mice.
F) FOS expression across vHPC layers in D2 mice.
G) FOS+ density in D1 and D2 cells across sex.
H) Density of D1 or D2 cells (GFP+) across sex.
I) Density of co-localized FOS and GFP expression across sex.

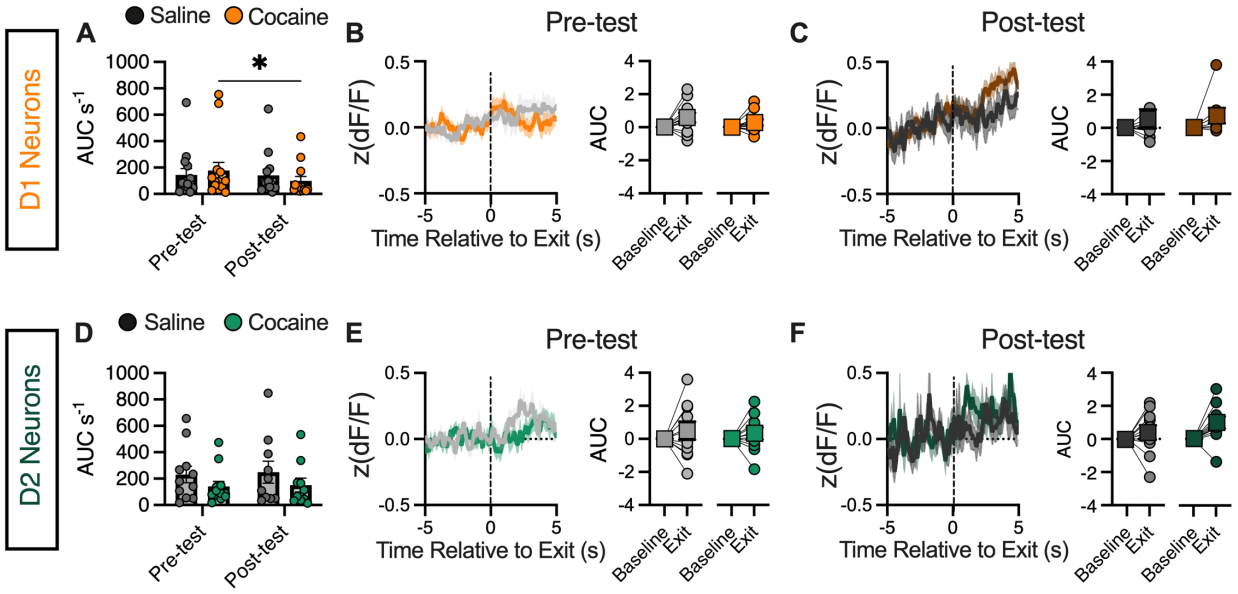

Fig. S2. Exit of saline- or cocaine-paired compartments during CPP has no effect on dopaminoceptive cell activity.

A) Area under the curve (AUC) of D1 activity while mice are in saline or cocaine-paired compartment (P=0.0242; 2-Way ANOVA).
B) Change in D1 signal when mice exit saline or cocaine paired side and resulting AUC.
C) Change in D1 signal when mice exit saline or cocaine paired side during post-test and AUC.
D) AUC of D2 activity while mice are in saline or cocaine-paired compartments.
E) Change in D2 signal when mice exit saline or cocaine paired side and resulting AUC.
F) Change in D1 signal when mice exit saline or cocaine paired side during post-test and AUC.

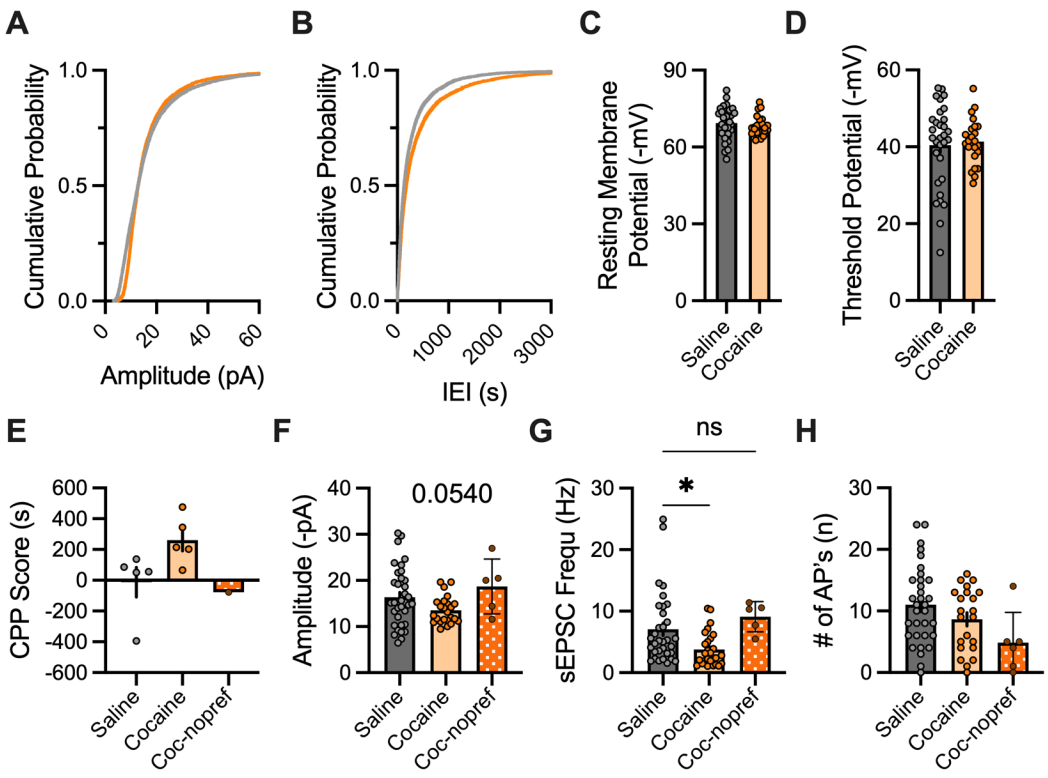

Fig. S3. Mice that do not form CPP do not show synaptic changes onto vHPC D1 cells.

A) Cumulative probability of sEPSC amplitude from D1-tdtomato cells in the vHPC.
B) Cumulative probability of sEPSC interevent interval (IEI).
C) Resting membrane potential.
D) Threshold potential.
E) CPP score.
F) sEPSC amplitude comparing data from Figure 2 with mouse that did not form preference.
G) sEPSC frequency comparing data from Figure 2 with mouse that did not form preference (P=0.0084; One-Way ANOVA).
H) Excitability at 80 pA current step injections comparing data from Figure 2 with mouse that did not form preference.

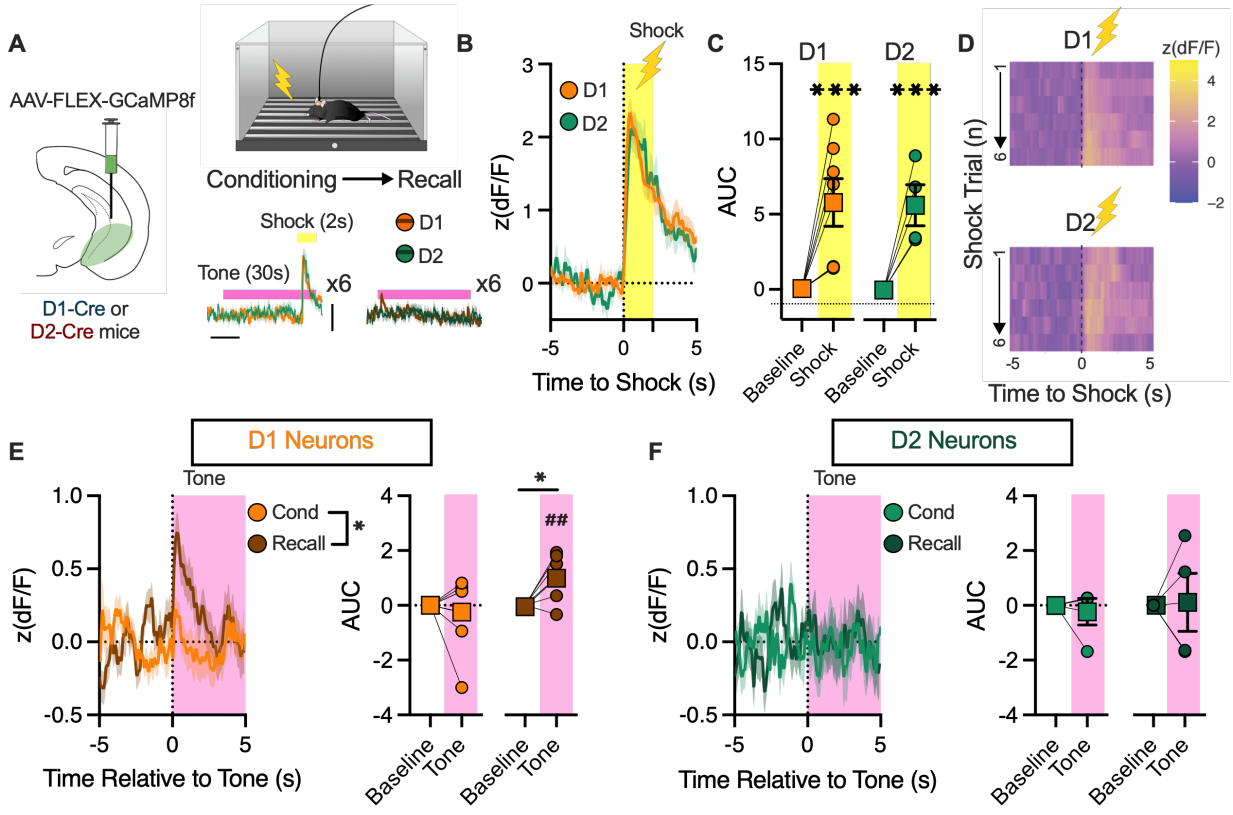

Fig. S4. D1 cells are inhibited by aversive conditioned cues.

A) Schematic of experimental design for fear conditioning experiments and representative D1 and D2 cell activity.

B) Average D1 and D2 responses to footshock.

C) Resulting average AUC following footshock (P_{Shock}=0.0010, 2-Way ANOVA).

D) Average heatmap of D1 (top) and D2 (bottom) responses to footshock across trial.

E) Change in D1 activity in response to tone during conditioning and recall (left) and resulting AUC (right) ($P_{Day \times Tone}$ = 0.04184, 2-Way ANOVA).

F) Change in D2 activity in response to tone during conditioning and recall (left) and resulting AUC (right) ($P_{Day \times Tone}$ = 0.8057).

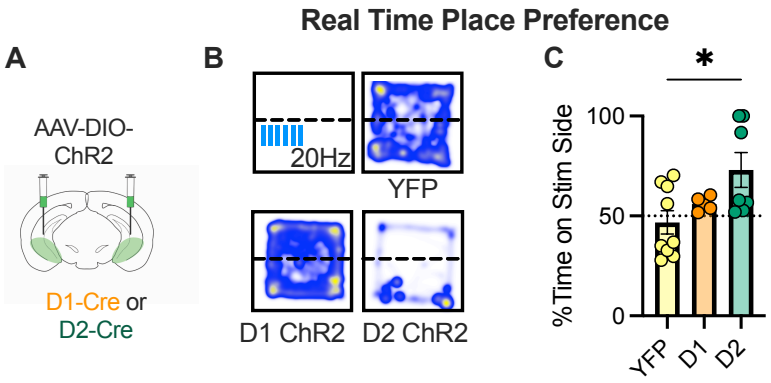

Fig. S5. Optogenetic activation of D2 cells is rewarding.

A) Schematic of optogenetic activation (YFP, *n*=9; D1-ChR2, *n*=5, D2-ChR2, *n*=7).

B) Representative heatmap of time spent in open field box during real time place preference.

C) Quantification of %time spent on side paired with optogenetic stimulation (P=0.0287, One-Way ANOVA).

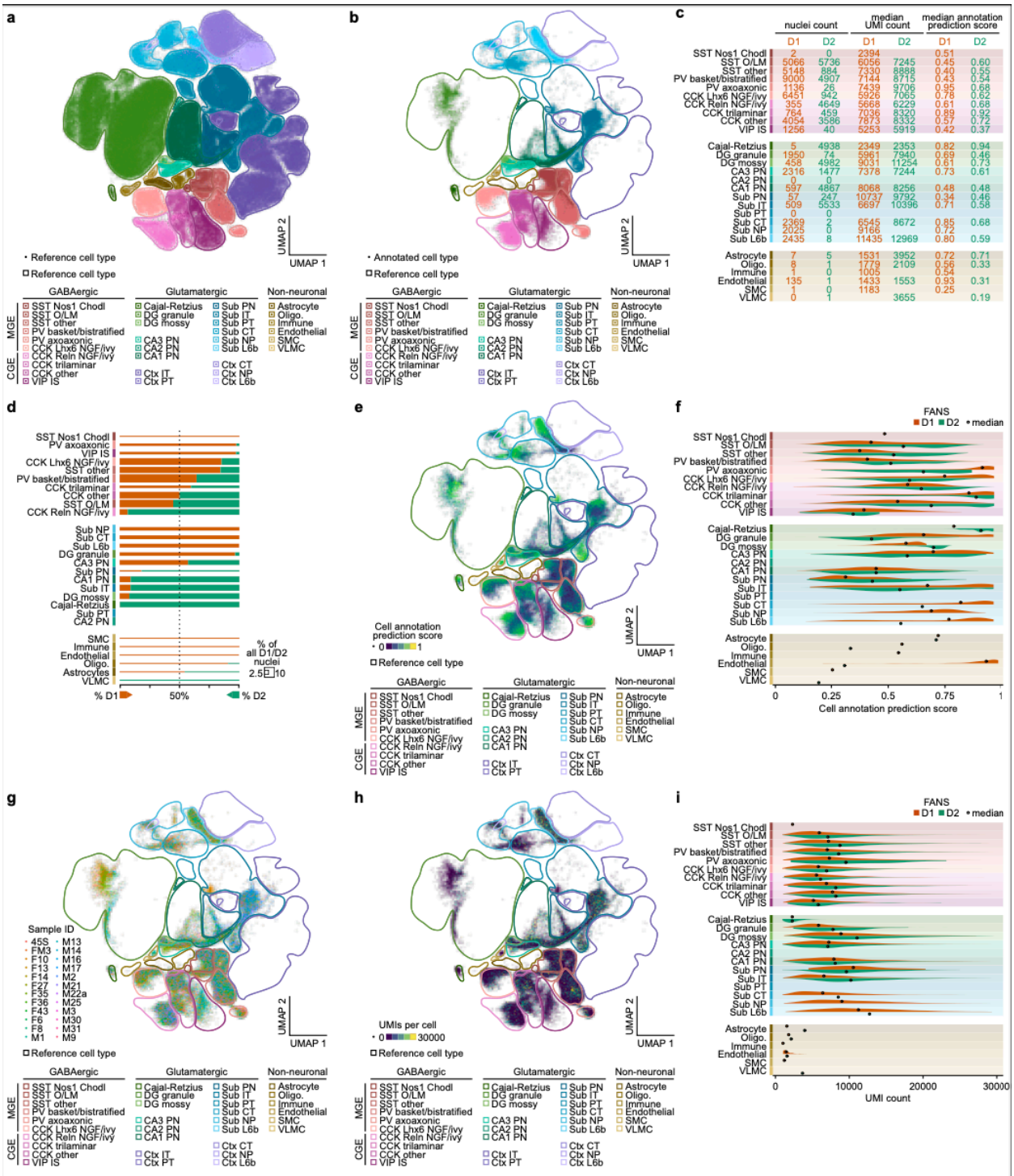

Fig. S6. Clustering vHPC D1 and D2 cells by use of snRNAseq.

A) UMAP of reference data set.
B) UMAP of sorted vHPC D1 and D2 cells using reference data set.
C) Prediction scores for annotated D1 and D2 cells using reference data set.
D) Proportion of D1 verse D2 cells across cell-type.
E) Prediction scores using reference data set to cluster cells.

F) Annotation prediction scores.
G) UMAP of cell distributions across sample.
H) UMAP of UMIs.
I) UMI count across cluster.

This clustering utilized Yao, et al. 2021[23] as the reference data set.

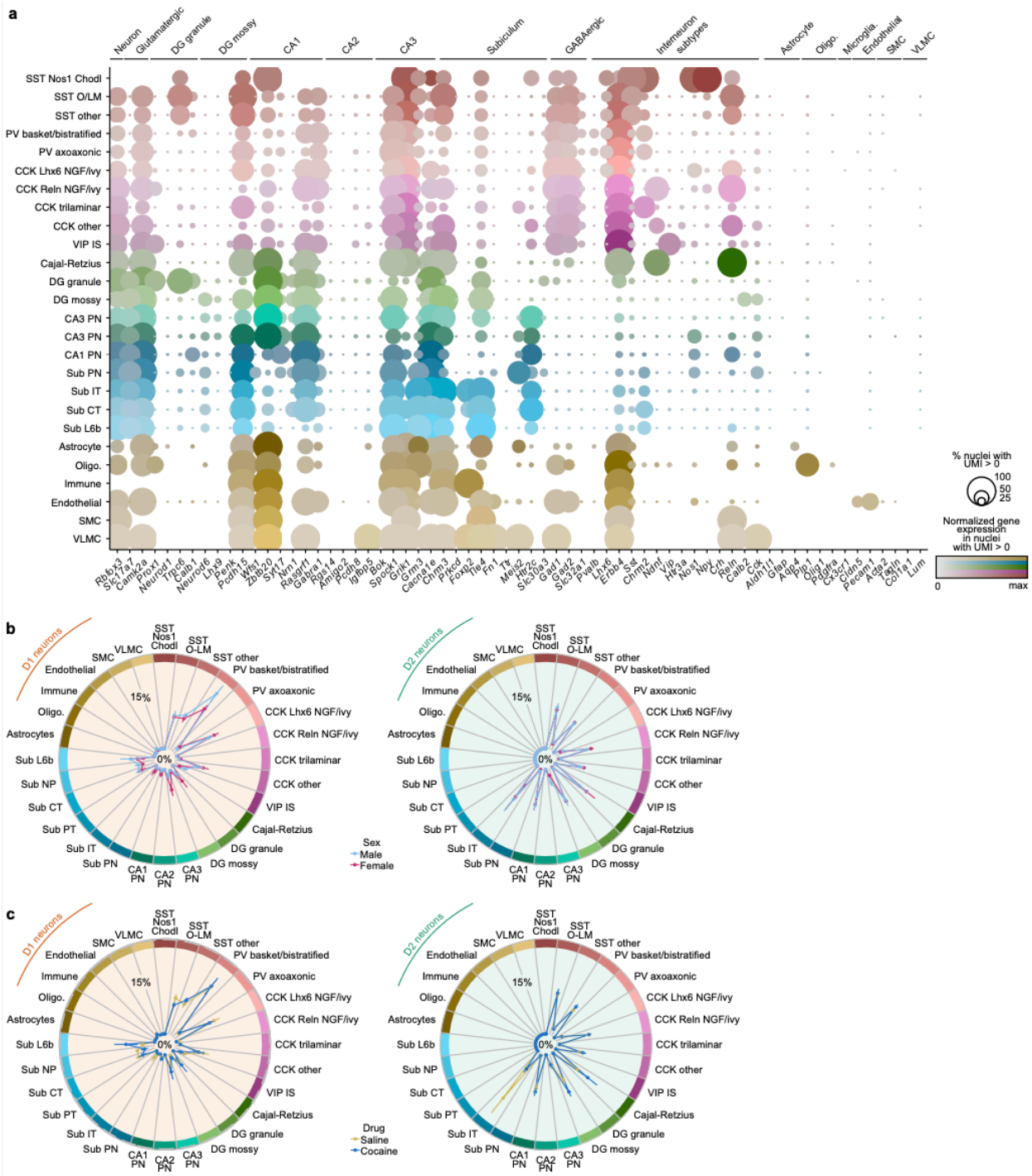

Fig. S7. Sex or treatment has no effect on proportion of cells across vHPC clusters.

A) vHPC subclusters and genes.

B) Proportion of D1 (left) and D2 (right) cells in subclusters across sex.

C) Proportion of D1 (left) and D2 (right) cells in subclusters across drug.

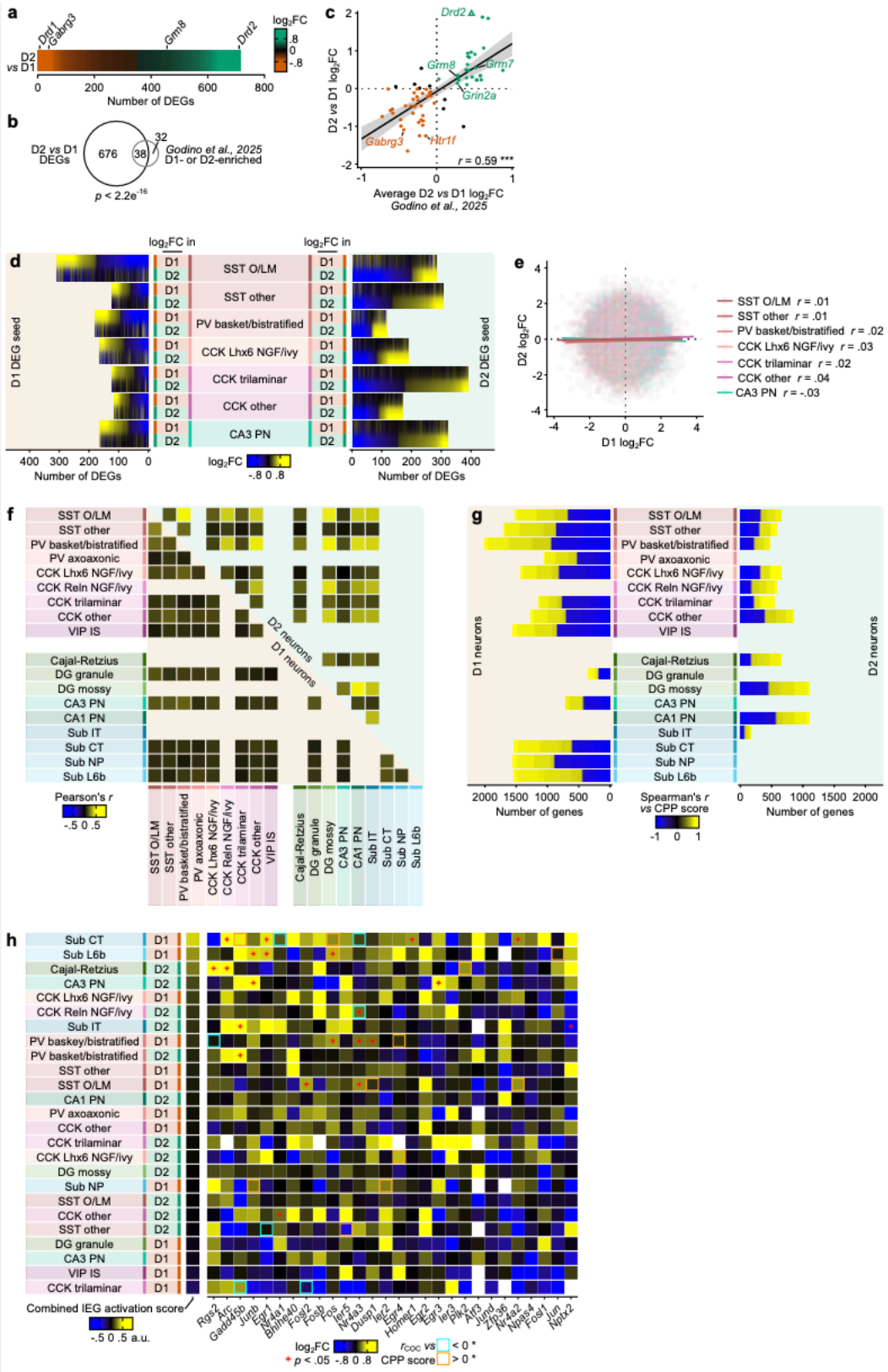
a
Drd1
Gabrg3
Grm8
Drd2
log2FC
.8
0
-.8
D2 vs D1
0
200
400
600
800
Number of DEGs
b
D2 vs D1 DEGs
676
38
32
Godino et al., 2025
D1- or D2-enriched
p < 2.2e-16
c
Drd2
Grm8
Grm7
Grin2a
Gabrg3
Htr1f
r = 0.59 ***
D2 vs D1 log2FC
Average D2 vs D1 log2FC
Godino et al., 2025
d
log2FC in
D1
D2
SST O/LM
SST other
PV basket/bistratified
CCK Lhx6 NGF/ivy
CCK trilaminar
CCK other
CA3 PN
D1 DEG seed
D2 DEG seed
Number of DEGs
log2FC
-.8 0 .8
e
D2 log2FC
D1 log2FC
SST O/LM r = .01
SST other r = .01
PV basket/bistratified r = .02
CCK Lhx6 NGF/ivy r = .03
CCK trilaminar r = .02
CCK other r = .04
CA3 PN r = -.03
f
SST O/LM
SST other
PV basket/bistratified
PV axoaxonic
CCK Lhx6 NGF/ivy
CCK Reln NGF/ivy
CCK trilaminar
CCK other
VIP IS
Cajal-Retzius
DG granule
DG mossy
CA3 PN
CA1 PN
Sub IT
Sub CT
Sub NP
Sub L6b
D2 neurons
D1 neurons
Pearson's r
-.5 0 .5
g
D1 neurons
D2 neurons
Number of genes
Spearman's r vs CPP score
-1 0 1
h
Combined IEG activation score
-.5 0 .5 a.u.
Rgs2
Arc
Gadd45b
Junb
Egr1
Nr4a1
Btg2
Fosl2
Fosb
Fos
Ier5
Nr4a3
Dusp1
Ier2
Egr4
Homer1
Egr2
Egr3
Ier3
Pik3
Atf3
Jund
Zfp36
Nr4a2
Npas4
Fosl1
Jun
Nptx2
log2FC
-.8 0 .8
p < .05
rcoc vs CPP score
< 0 *
> 0 *

Fig. S8. D1 and D2 vHPC cells represent distinct cell types, yet cocaine-activated gene patterns are conserved across dopaminoceptive cell identity.

A) Heatmap of DEGs comparing D1 vs. D2.
B) Comparison to previously published DEGs between D1 and D2.
C) Correlations with dataset obtained here to previously published[15].
D) Heatmap of log2foldchange comparing D1 and D2 DEGs.
E) Correlations of changes in gene expression between D1 and D2 subclusters.
F) Correlations of gene changes induced by cocaine CPP in D1 and D2 clusters.
G) Number of DEGs correlated with CPP score.
H) Immediate early gene (IEG) induction following cocaine CPP in D1 and D2 subclusters and correlations with CPP score.